

Novel method of preparing hydroxyapatite foams

Anushini Muthutantri · Jie Huang ·
Mohan Edirisinghe

Received: 8 September 2007 / Accepted: 4 January 2008 / Published online: 24 January 2008
© Springer Science+Business Media, LLC 2008

Abstract Porous scaffolds are considered a key strategy in the concept of bone tissue engineering. Hydroxyapatite, which is a bioceramic has been used as a popular scaffold material due to its bioactive and osteoconductive properties. A combination of slurry-dipping and electrospraying has been used as a new foam fabrication method to produce porous and interconnected foam structures. The combined method has shown to overcome the shortcomings of the individual methods and it has produced open pores in the desired range of 100–350 μm . The porosity which was determined by calculation and microtomography was between 84% and 88%. Reduced cracks and thicker struts were observed in the microstructure, pointing to improved mechanical properties.

1 Introduction

Bone tissue engineering (TE) has become one of the key areas of research as a successful treatment option for bone regeneration [1]. Scaffolds are used in tissue engineering to direct tissue development and for bone tissue engineering, open pore scaffolds with a pore size range of 100–350 μm and porosity greater than 90% are preferred [2]. Hydroxyapatite (HA), which is a ceramic and similar in composition to the inorganic component of bone, is also known for its osteoconductivity and bioactivity [3]. HA has been used in dental and orthopaedic surgery as bone defect fillers and as coatings on metallic implant surfaces, to enhance bone

regeneration [4, 5]. HA has been investigated as a potential scaffold material for bone tissue engineering applications to promote osteoblast differentiation and proliferation [6].

Nano-sized HA (nHA) particles have a resemblance to the morphology of the mineral crystals found in bone and hence have the potential to enhance the mechanical properties of implants and their osteoconductivity [7, 8]. Replication or slurry dipping is a simple and popular method of producing porous and interconnected foams using a ceramic slurry and has been used to produce HA scaffolds [9–11]. This method produces scaffolds with poor mechanical properties due to the presence of the central void in the strut and the presence of micropores and microcracks due to non-uniform coating of the ceramic slurry [12]. Electrospraying is another form of replication method that can produce interconnected pore structures and it has been possible to obtain solid struts with no central hole [13], therefore leading to improved mechanical properties [14]. However, foam preparation by electrospraying only, requires well dispersed ceramic suspensions of high concentrations of 60–65 wt.% [13, 14].

In this study, a combination of slurry dipping and electrospraying is explored to produce interconnected pore networks with pores within the desired range to overcome the limitations when each method is used individually. A comparison has been made of the sintered foams that have been prepared using replication (dipping), spraying and a combination of both methods based on their porosity and microstructures.

2 Materials and methods

Polyurethane (PU) templates with fully reticulated pore structure of cell size range 740–1040 μm were obtained

A. Muthutantri · J. Huang · M. Edirisinghe (✉)
Department of Mechanical Engineering, University College
London, Torrington Place, London WC1E 7JE, UK
e-mail: m.edirisinghe@ucl.ac.uk

from Recticel (Corby, UK). The polymer templates were cut into 5 mm × 5 mm × 10 mm dimensions. Two nHA suspensions, 18 wt.% (water-based) and 6 wt.% (ethanol-based) were used. The latter suspension was a modified version of the former and ethanol was added to enable the suspension to be electrospayed.

2.1 Replication method

Nano-HA suspension of 18 wt.% (water based) was used. The PU templates were immersed in the slurry for ~5 min, the excess slurry was squeezed out.

2.2 Electrospaying

The 6 wt.% ethanol-based nHA suspension was used for electrospaying. The experimental set-up shown in Fig. 1 was used for electrospaying and a stainless steel needle of orifice diameter 510 μm was used. A flow rate of 1.67×10^{-10} m³/s and voltage in the range of 4.1–5.5 kV were the conditions at which a stable cone-jet was established and was observed using a high-speed camera. The stable cone-jet mode enables controlled jet and droplet generation, with near-monodisperse droplets [15] usually <<50 μm in size [16]. A mechanical arm which was also the ground electrode, was used to rotate the foam to ensure uniform coating of the HA suspension. The samples were electrospayed for 2 h.

2.3 Combined method of dipping and electrospaying

The templates were immersed in the 18 wt.% nHA suspension for 5 min, excess was squeezed out and was immediately followed by electrospaying for 30 min and 1 h time intervals.

The ceramic coated templates were allowed to dry for ~12 h. All air-dried samples were heated to 400°C, maintained at that temperature for 1 h for pyrolysis of the template and then sintered to a maximum temperature of 1200°C. The sintered samples were soaked at the maximum temperature for 5 h prior to being cooled down to ambient temperature. The heating and cooling rates were set to 2°C/min and 5°C/min, respectively.

3 Sample characterisation

3.1 Porosity measurement

3.1.1 Calculation

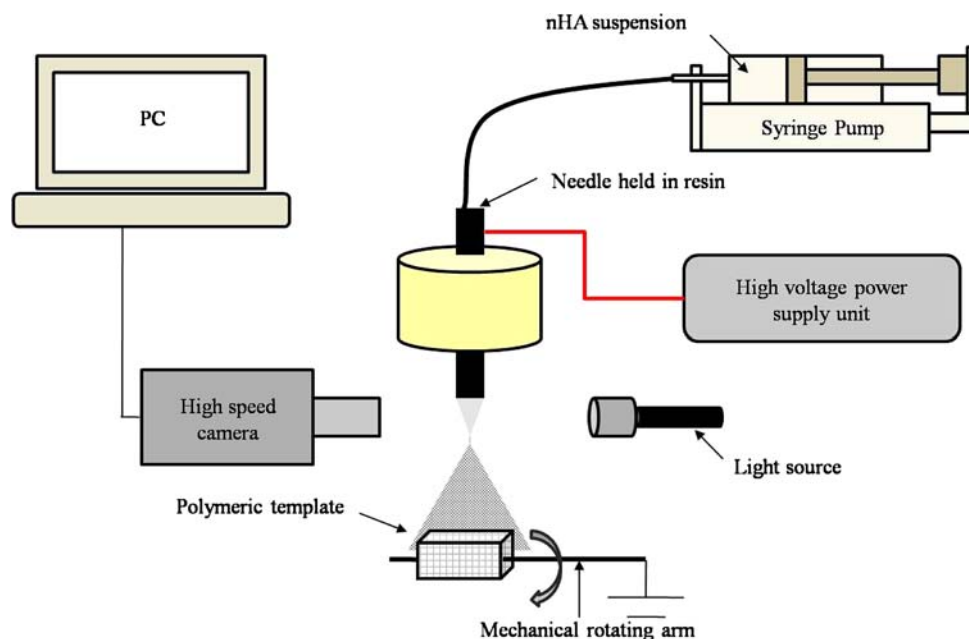
The porosity p of the foam was calculated by [17]

$$p = 1 - \frac{\rho_{foam}}{\rho_{solid}} = 1 - \rho_{relative} \quad (1)$$

where the density of solid HA; $\rho_{solid} = 3156 \text{ kgm}^{-3}$ [18].

The density ρ_{foam} of the HA scaffolds was determined from the mass and dimensions of the sintered structures. Six samples for each experimental condition were analysed and average values were obtained.

Fig. 1 Equipmet set-up for electrospaying



3.1.2 X-ray microtomography (X μ T)

Internal pore network for the different foam fabricating combinations were compared using Sky-Scan 1072 X-ray microtomograph. The porosity of the reconstructed 3D images were analysed and calculated using the CTAn software.

3.2 Microstructural analysis

The microstructures of the sintered foams were characterised using a Hitachi S-3400N scanning electron microscope (SEM). The samples were sputter coated with gold and were observed using an accelerating voltage of 20 kV. Both the outer and inner surfaces of the foams were imaged to investigate the uniformity of the sintered structures. Approximately 100 measurements were averaged from ten samples for both pore size and strut thickness to obtain an accurate distribution of values.

4 Results and discussion

The distance between the exit of the needle and the foam surface was optimised to 10 mm to obtain maximum coverage of the nHA coating. The flow rate is an important parameter and can significantly influence the production of droplets. There usually exists a minimum and maximum flow rate for a given suspension to obtain a stable cone-jet and are usually imposed experimentally. Within this stable flow rate range, relatively higher flow rates produce relatively larger droplets [19] that tend to be polydisperse, but with a higher production frequency [20]. Relatively lower flow rates within the stable cone-jet range are known to produce finer and near-monodisperse droplets and is usually

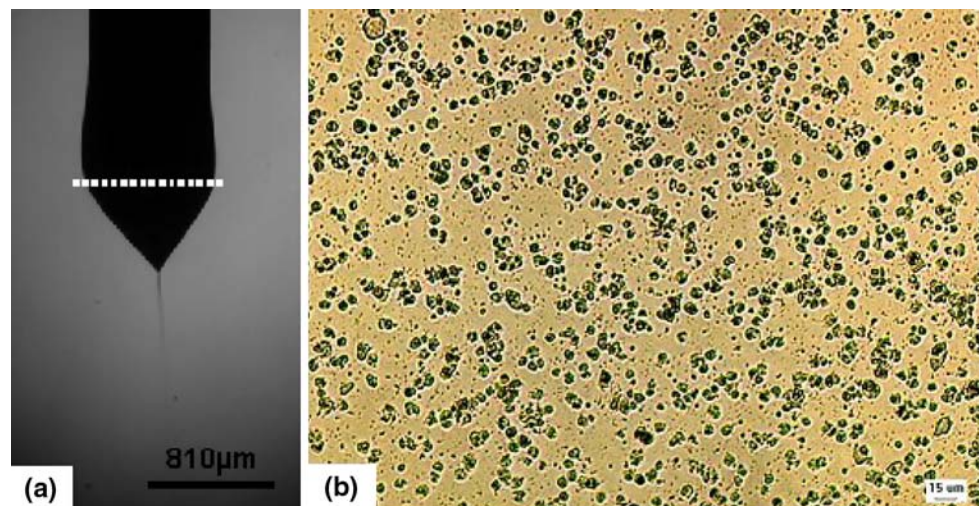
utilised for nano-particle fabrication and mass spectroscopy [21]. For this study, the flow rate was optimised to $1.67 \times 10^{-10} \text{ m}^3/\text{s}$, and the cone-jet mode established in electro spraying produced sufficiently fine droplets ($<15 \mu\text{m}$ in diameter (optical microscopy)) of the nHA suspension to enable penetration into the template (Fig. 2).

The rotating arm was operated by a multi-ratio motor gear box. The rotating speed was changed by altering the gear-sets. The minimum speed which was considered was 2 rotations/min (rpm) which was too slow and the maximum speed was set to 115 rpm which seemed too fast. It was not possible to obtain a uniform coating of the ceramic suspension using either of the above speeds and it was set to 29 rpm which resulted in satisfactory coverage of the polymeric template by the nHA suspension.

The porosity of the foams was calculated using Eq. 1. These values had a large standard deviation, because the mass and dimensions of the samples showed a large variation and therefore were only an estimate due to the non-uniformity of the porous foams (Fig. 3). These values were compared with the values obtained using the reconstructed three-dimensional images from X μ T, which gives a much smaller standard deviation and can be considered to be more accurate as it considers the internal porosity of the structures. The average porosity levels for all structures were between 84% and 94% (Fig. 3) which are favourable characteristics for scaffolds to be used for tissue engineering of bone.

The microstructures were analysed using the SEM to observe the strut structure and pore interconnectivity, both on the surface and the cross-sections of the sintered foams (Fig. 4). The dipping method produced interconnected pores both on the surface and in the cross-section (Fig. 4a, b), but there were microcracks along the length of the struts which will compromise its mechanical properties. The structures obtained by electro spraying did not show much interconnectivity on the sprayed surface (Fig. 4c), but were found to

Fig. 2 (a) Cone-jet mode of 6 wt.% nHA suspension used for electro spraying and (b) optical microscopy image showing near-monodisperse HA droplets of diameter $<15 \mu\text{m}$ produced in electro spraying (The dotted line in (a) indicates the exit of the needle)



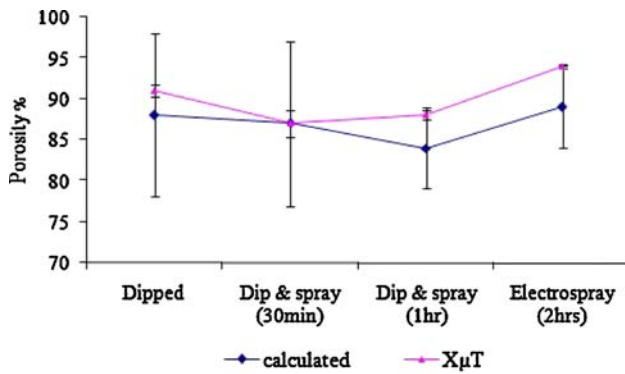
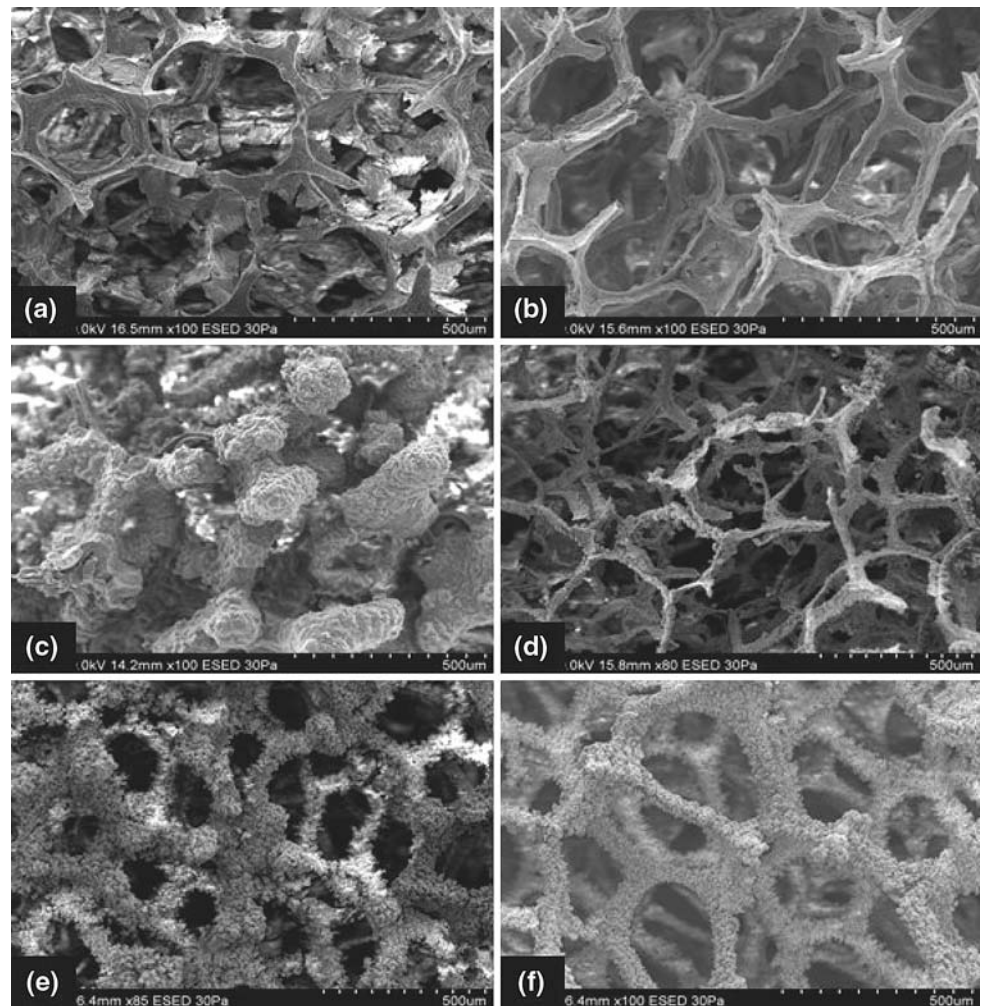


Fig. 3 Comparison of porosities between the calculated values and the microtomography ($X\mu T$) values. The porosity was calculated using six samples and for $X\mu T$, 350 sections were analysed. The former has a standard deviation of <10 and the latter, a value of <1.6

be rather porous on the innermost surface (Fig. 4d). An interconnected pore network was present on the inner and outer surfaces of the structures prepared using the combined method of dipping and electro spraying (Fig. 4e, f).

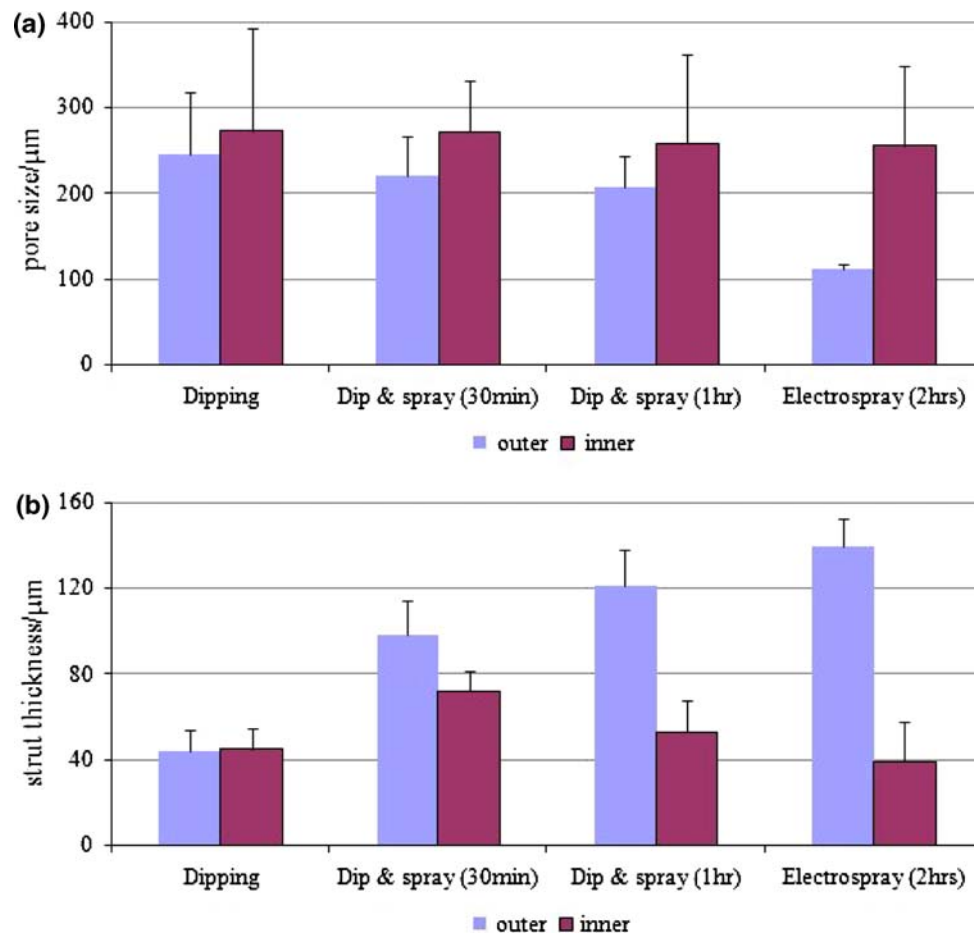
Fig. 4 Scanning electron micrographs showing the strut structure and pore interconnectivity both on the surface and the cross sections of the sintered foams [*Dipped*: (a) surface, (b) cross-section; *Electro spray* (2 h): (c) surface, (d) cross-section; *Dip and spray* (30 min): (e) surface, (f) cross-section]



The variation of average pore sizes and strut thickness on the outer and inner surfaces of the sintered foams are shown in relation to the foam fabricating method in Table 1. The distribution of pore size and strut thickness was homogeneous in the dipped samples (Fig. 5). The pore size on the outer surface was observed to be smaller than on the inner surface for the foam structures prepared by using electro spraying and combined methods, and could be due to the thicker struts observed on the outer surface (Fig. 5b). The thickness of the struts increases with spraying time due to increased deposition of HA droplets onto the template. Electro spraying only produced the smallest pores on the surface and the pore size was increased towards the centre of the foam. The struts inside the foam were reduced by $\sim 70\%$ in thickness in comparison to the struts on the sprayed surface of the scaffold. This is due to the agglomerated HA particles on top of the foam reducing penetration of the slurry into the foam resulting in a weak centre, which could result in poor mechanical properties. The combined method of dipping and electro spraying produced foam structures having pore

Table 1 Comparison of the change in pore size and strut thickness by varying the fabrication method ($n = 100$)

Sample label	Pore size (outer)/ μm	Pore size (inner)/ μm	Strut thickness (outer)/ μm	Strut thickness (inner)/ μm
Dipping	245 ± 70	273 ± 120	44 ± 10	45 ± 10
Dip & spray (30 min)	220 ± 50	272 ± 60	98 ± 20	72 ± 10
Dip & spray (1 h)	208 ± 40	259 ± 100	121 ± 20	53 ± 15
Electrospray (2 h)	111 ± 10	255 ± 90	140 ± 15	39 ± 20

**Fig. 5** Comparison of (a) pore size and (b) strut thickness of the sintered structures obtained using different methods. Approximately 100 measurements were averaged from ten samples for each category

sizes within the desired range of 100–350 μm and they were open pores with good interconnectivity.

5 Conclusions

A novel method of fabricating HA scaffolds has been introduced; a combination of slurry-dipping and electro-spraying. This method is capable of producing open and interconnected pore structures with thicker struts. The pores are in the range of 100–350 μm , thus meeting the requirement for bone TE scaffolds. The polymeric template

is coated by the dipping method and the fine droplets produced by electro-spraying reduce the microcracks and thickens the struts. Therefore, improved mechanical reliability of these foams can be expected, and an in depth study of the process is under investigation.

Acknowledgements Authors would like to thank Jenny Robinson and Dr. Serena Best (Department of Materials Science and Metallurgy, University of Cambridge) for the preparation of the original 18 wt.% nHA suspension, and Dr. Pete Laity (University of Cambridge) for assistance with microtomography imaging. EPSRC grants: GR/S 97880, GR/S 97873 and the Royal Society, UK (Brian Mercer Fund) are gratefully acknowledged for their support in funding the research.

References

1. K.J.L. Burg, S. Porter, J.F. Kellam, *Biomaterials* **21**, 2347 (2000)
2. H. Yoshimoto, Y.M. Shin, H. Terai, J.P. Vacanti, *Biomaterials* **24**, 2077 (2003)
3. L.L. Hench, *J. Am. Ceram. Soc.* **74**, 1487 (1991)
4. S.S. Kim, M.S. Park, O. Jeon, C.Y. Choi, B.S. Kim, *Biomaterials* **27**, 1399 (2006)
5. X. Miao, Y. Hu, J. Liu, A.P. Wong, *Mater. Lett.* **58**, 397 (2004)
6. H.I. Shin, K.H. Kim, I.K. Kang, K.S. Oh, *Key Eng. Mater.* **288–289**, 245 (2005)
7. G.B. Wei, P.X. Ma, *Biomaterials* **25**, 4749 (2004)
8. C. Du, F.Z. Cui, X.D. Zhu, K. De Groot, *J. Biomed. Mater. Res.* **44**, 407 (1999)
9. H.W. Kim, J.C. Knowles, H.E. Kim, *J. Mater. Sci.: Mater. Med.* **16**, 189 (2005)
10. J.T. Tian, J.M. Tian, *J. Mater. Sci.* **36**, 3061 (2001)
11. Y. Abdullah, M.R. Yusof, I. Besar, R. Mustafa, K.A. Hing, *Key Eng. Mater.* **206–213**, 1543 (2001)
12. J.M. Tulliani, L. Montanaro, T.J. Bell, M.V. Swain, *J. Am. Ceram. Soc.* **82**, 961 (1999)
13. S.N. Jayasinghe, M.J. Edirisinghe, *J. Porous Mater.* **9**, 265 (2002)
14. Q.Z. Chen, A.R. Boccaccini, H.B. Zhang, D.Z. Wang, M.J. Edirisinghe, *J. Am. Ceram. Soc.* **89**, 1534 (2006)
15. J. Rosell-Llompart, J. Fernández de la Mora, *J. Aerosol. Sci.* **25**, 1093 (1994)
16. A. Jaworek, A. Krupa, *J. Aerosol Sci.* **30**, 873 (1999)
17. L.J. Gibson, M.F. Ashby, *Cellular solids, Structure and Properties*, 2nd edn. (Cambridge University Press, UK, 1997) p. 15
18. L.L. Hench, S.M. Best, in *Biomaterials Science: an Introduction to Materials in Medicine*, 2nd edn. ed. by D. Ratner, F.J. Schoen, A.S. Hoffman, J.E. Lemons (Elsevier Academic Press, 2004) pp. 3–170
19. A.M. Ganán-Calvo, J. Davila, A. Barrero, *J. Aerosol Sci.* **28**, 249 (1997)
20. F.J. Higuera, *J. Fluid Mech.* **484**, 303 (2003)
21. J.M. Grace, J.C.M. Marijnissen, *J. Aerosol Sci.* **25**, 1005 (1994)